Kosambi-Cartan-Chern Stability in the Intermediate Nonequilibrium Region of the Brusselator Model

Yamasaki, Kazuhito

Yajima, Takahiro

International Journal of Bifurcation and Chaos

Kosambi-Cartan-Chern stability in the intermediate non-equilibrium region of the Brusselator model

Kazuhito Yamasaki
Department of Planetology, Graduate School of Science, Kobe University, Nada, Kobe 657-8501, Japan
yk2000@kobe-u.ac.jp

Takahiro Yajima
Department of Mechanical Systems Engineering, Faculty of Engineering, Utsunomiya University, Utsunomiya, 321-8585, Japan
yajima@cc.utsunomiya-u.ac.jp

Received (to be inserted by publisher)

This study applies the Kosambi-Cartan-Chern (KCC) theory to the Brusselator model to derive differential geometric quantities related to bifurcation phenomena. Based on these geometric quantities, the KCC stability of the Brusselator model is analyzed in linear and nonlinear cases to determine the extent to which non-equilibrium affects bifurcation and stability. The geometric quantities of the Brusselator model have a constant value in the linear case, and are functions of spatial variables with parameter dependence in the nonlinear case. Therefore, the KCC stability of the nonlinear case shows various distribution patterns, depending on the distance from the equilibrium point (EQP), as follows: in the regions near or far enough from the EQP, the distribution of KCC stability is uniform and regular; and in the intermediate non-equilibrium region, the distribution varies and shows complex patterns with parameter dependence. These results indicate that stability in the intermediate non-equilibrium region plays an important role in the dynamic complex patterns in the Brusselator model.

Keywords: Jacobi stability; KCC theory; bifurcation theory; Brusselator model; non-equilibrium; differential geometry

1. Introduction

Bifurcations are key factors in the spontaneous emergence of temporal organization in nonlinear systems [Thompson, 1982]. The Belousov-Zhabotinsky reaction is a classic example of such self-organizing phenomena [Belousov, 1959; Zhabotinnsky, 1964; Prigogine, & Lefever, 1968; Nicolis, & Prigogine, 1977; Taylor, 2002]. The Brusselator model, one of the simplest models to exhibit this phenomenon, comprises two first-order differential equations (e.g., [Nicolis, & Prigogine, 1977; Lavrova *et al.*, 2009; Luo, & Guo, 2018; Rech, 2019; Deng, & Zhou, 2020; Qin *et al.*, 2020]):

$$\partial_t X = A - (B+1)X + X^2 Y, \tag{1}$$

$$\partial_t Y = BX - X^2 Y, \tag{2}$$

where X and Y are real-valued functions, and A and B are positive parameters. This can be rewritten according to changes in concentration from the primary values, $X = A + x$ and $Y = B/A + y$, as follows

[Thompson, 1982]:

$$\dot{x} = (B-1)x + A^2 y + \frac{Bx^2}{A} + 2Axy + x^2 y, \tag{3}$$

$$\dot{y} = -Bx - A^2 y - \frac{Bx^2}{A} - 2Axy - x^2 y. \tag{4}$$

From Eqs. (3) and (4), the equilibrium point (EQP) is given by $(x, y) = (0, 0)$.

Bifurcation analysis of the stability of the Brusselator model has generated much interest in the self-organization of non-equilibrium chemical systems, i.e., dynamic phenomena in reacting systems far from equilibrium (e.g.,[Nicolis, & Prigogine, 1977; Ma, & Hu, 2014; Freire *et al.*, 2017; Zhao, & Ma, 2019]). Given the importance of stability under non-equilibrium conditions, the degree to which non-equilibrium affects stability must be considered. In this paper, we consider whether the stability of bifurcation phenomena becomes more complex as the system moves away from the equilibrium state.

We applied the Kosambi-Cartan-Chern (KCC) theory to quantify the effect of bifurcation on stability in the non-equilibrium region (e.g., [Yamasaki & Yajima, 2020]). The KCC theory was first applied to the study the geometric invariance of second-order ordinary differential equations [Kosambi, 1933; Cartan, 1933; Chern, 1939; Antonelli *et al.*, 1993]. Recently, it has also been used in the analysis of stability (e.g., [Antonelli, & Bucataru, 2003; Sabău, 2005a; Udriste & Nicola, 2009; Neagu, 2013; Harko *et al.*, 2016]). Our previous KCC analyses of typical bifurcations (saddle-node, transcritical, and pitchfork bifurcations) showed that stability varies in the non-equilibrium region [Yamasaki & Yajima, 2017, 2020]. Here, KCC theory is applied to the Brusselator model, described by Eqs. (3) and (4), to evaluate the degree to which non-equilibrium affects stability. To interpret the results clearly, the Brusselator model is analyzed separately as linear and nonlinear cases.

The structure of this paper is as follows. In Section 2, we provide a brief review of KCC theory. In Section 3, based on KCC theory, we derive the geometric quantities of Eqs. (3) and (4) in the linear case, and compare the results with those of previous linear stability analyses. In Section 4, we derive geometric quantities in the nonlinear case and consider KCC stability in the non-equilibrium region. Our conclusions are presented in Section 6.

2. KCC theory applied to a system comprising two first-order differential equations

2.1. *Basic theory*

As mentioned in the Introduction, KCC theory has been used to analyze the geometric structure of differential equations. Because a dynamic system is often described by differential equations, KCC theory has been applied to the geometric aspects of various dynamic structures, including those of physical (e.g., [Kumar *et al.*, 2019; Krylova *et al.*, 2019; Alawadi *et al.*, 2020; Liu *et al.*, 2020; Klën, & Molina, 2020]), biological (e.g., [Antonelli *et al.*, 1993; Yamasaki & Yajima, 2013; Antonelli *et al.*, 2014; Antonalli *et al.*, 2019; Kolebaja, & Popoola, 2019]) and general (e.g., [Gupta, & Yadav, 2017; Chen, & Yin, 2019; Gupta *et al.*, 2019; Gupta, & Yadav, 2019]) systems. Moreover, it has been applied in mathematics to resolve the inverse problem of updating the general parameters of dynamic systems [Sulimov *et al.*, 2018], and the geometric parameters of complex systems, including chaotic ones (e.g., [Oiwa, & Yajima, 2017; Huang *et al.*, 2019; Chen *et al.*, 2020; Feng *et al.*, 2020; Liu *et al.*, 2021]).

The main component of KCC theory is a second-order ordinary differential equation [Kosambi, 1933; Cartan, 1933; Chern, 1939], e.g., equations of motion. In analytical mechanics, equations are obtained from two first-order differential equations. In this case, a single second-order equation can be derived by combining the two first-order equations. The Brusselator model considered in this paper comprises two first-order differential equations (3) and (4). These are then combined into a single second-order differential equation, to which the theory of KCC can be applied. The analysis methods are described in the following.

Let us consider the following system comprising two first-order differential equations for $x = x(t)$ and

$y = y(t)$:

$$\dot{x} = f_x(x, y), \tag{5}$$

$$\dot{y} = f_y(x, y), \tag{6}$$

where $f_x(x, y)$ and $f_y(x, y)$ are smooth functions. Equation (5) can be rewritten as $y = h(x, \dot{x})$. Substitution of this equation into Eq. (6) gives the following second-order differential equation:

$$\ddot{x} + g_x(x, \dot{x}) = 0, \tag{7}$$

where $g_x(x, \dot{x})$ is a smooth function. The form $\ddot{y} + g_y(y, \dot{y}) = 0$ can be derived in a similar way. In the linear case, there is no difference in stability between x and y. Details are given in the following sections.

As a simple example, let us consider the Lotka-Volterra predation system. In Eqs. (5) and (6), $f_x = rx - axy$ and $f_y = bxy - cy$, where r, a, b, c are all positive parameters. Therefore, $h = (rx - \dot{x})/(ax)$ and we can obtain $g_x = rx(bx - c) + \dot{x}(c - bx) - (\dot{x}^2)/x$ using Eq. (7).

According to KCC theory, a small perturbation $u_x\delta\tau$ in the trajectory of Eq. (7) gives the covariant form of the variational equation $D^2u_x/Dt^2 = P_x u_x$, where $D(\cdots)/Dt$ is a covariant differential, and the initial conditions are given by $u_x(0) = 0$ and $\dot{u}_x(0) \neq 0$ (e.g., [Antonelli, & Bucataru, 2003]). P_x is the geometric object, referred to as the deviation curvature tensor and defined by the following relation (e.g., [Antonelli, & Bucataru, 2003]):

$$P_x = -\frac{\partial g_x}{\partial x} + \frac{\partial N_x}{\partial x}\dot{x} - G_x g_x + (N_x)^2, \tag{8}$$

N_x is a coefficient related to the nonlinear connection:

$$N_x = \frac{1}{2}\frac{\partial g_x}{\partial \dot{x}}, \tag{9}$$

and G_x is a Berwald connection:

$$G_x = \frac{\partial N_x}{\partial \dot{x}}. \tag{10}$$

When Eqs. (5) and (6) are linear systems, the geometric quantities defined above are all constant. On the other hand, in the nonlinear system, the geometric quantities are functions of x and y. As described in the next section, these geometric quantities are related to system stability. Thus, stability in the nonlinear system varies within (x, y)-space. This paper considers stability in the linear and the nonlinear cases described in Sections 3 and 4, respectively.

2.2. *N-stability and J-stability*

The deviation curvature (8) determines the Jacobi stability of the system, i.e., the robustness of its trajectory[Lake & Harko, 2016; Sabău, 2005a; Salnikova *et al.*, 2020]. The trajectory of a one-dimensional system is Jacobi stable when $P < 0$, and Jacobi unstable when $P \geq 0$ [Antonelli, & Bucataru, 2003; Sabău, 2005a,b]. In this paper, we refer to the system as J-stable when $P < 0$, and as J-unstable when $P \geq 0$. Moreover, we consider the nonlinear connection (9), as this is also related to the stability of the system ([Yamasaki & Yajima, 2013, 2016]). Also, we refer to the system as being N-stable when $N > 0$, as N-unstable when $N < 0$, and as N-neutral when $N = 0$.

Around the EQPs, J-stable and J-unstable correspond to a spiral and a node, respectively [Sabău, 2005a]. N-stable, N-unstable, and N-neutral correspond to linear stable, linear unstable, and neutral, respectively ([Yamasaki & Yajima, 2013, 2016]). For instance, J-stable and N-stable around the EQP correspond to a stable spiral. The relationship between the stability type (according to bifurcation theory) and geometric terms (according to KCC theory) around the EQPs is summarized in Fig. 1 [Yamasaki & Yajima, 2013].

The relationship between KCC stability and other types of stability, such as Lyapunov stability, is reviewed in [Abolghasem, 2013b]. Finally, we highlight the differences between the Jacobi stability and other stability definitions, such as Lyapunov and orbital stability. [Abolghasem, 2013b] explicitly showed

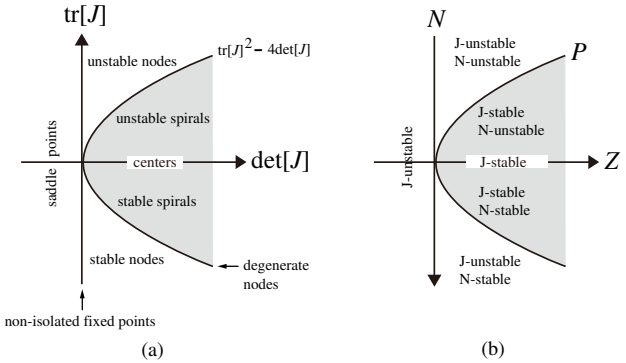

Fig. 1. Type and stability of equilibrium points (EQPs) adapted from Yamasaki and Yajima (2013). (a) Diagram showing a Jacobian J of the linearized system around the EQPs. (b) Diagram showing geometric quantities based on the Kosambi, Cartan, and Chern (KCC) theory. Note that the N-axis is reversed. From Yamasaki and Yajima (2013), $N = -(1/2)\mathrm{tr}[J]$, $Z = \det[J]$ and $P = N^2 - Z$.

that the stability derived from Lyapunov analysis is the same as the Jacobi stability for a Hamiltonian system with one degree of freedom. Abolghasem also showed that these stability concepts agree in three cases of torque-free rigid body motion around a stationary point, circular orbits in a central force field, and circular orbits in Schwarzschild spacetime [Abolghasem, 2012a,b, 2013a]. [Boehmer *et al.*, 2010] analyzed the relationship between the Jacobi and linear Lyapunov stability of dynamical systems in the fields of gravitation and astrophysics and show that there are cases in which the Lyapunov stability and the Jacobi stability do not agree. Few studies have examined the relationship between KCC theory and orbital stability, although asymptotical orbital stability is considered in predation and herbivory ecosystems [Antonelli, & Kazarinoff, 1984].

3. KCC analysis: linear case of the Brusselator model

3.1. *Geometric quantities*

Stability analysis based on Eqs. (3) and (4) is often applied to the linear case. In this section, we also apply KCC theory to the linear case, and compare the results with those obtained previously.

When we ignore the nonlinear terms, Eqs. (3) and (4) can be rewritten as

$$\dot{x} = (B-1)x + A^2 y, \tag{11}$$

$$\dot{y} = -Bx + A^2(-y). \tag{12}$$

Let us apply KCC theory to Eqs. (11) and (12) based on the method described in Section 2.1. First, we rewrite (11) for y:

$$y = h(x, \dot{x}) = \frac{-Bx + \dot{x} + x}{A^2}. \tag{13}$$

Substitution of Eq. (13) in Eq. (12) leads to

$$\ddot{x} + g_x(x, \dot{x}) = 0, \tag{14}$$

with

$$g_x(x, \dot{x}) = \left(A^2 - B + 1\right)\dot{x} + A^2 x. \tag{15}$$

Given g_x, Eqs. (9), (10), and (8) provide the geometric quantities of the Brusselator model in the linear case:

$$N_x = \frac{1}{2}\left(A^2 - B + 1\right), \tag{16}$$

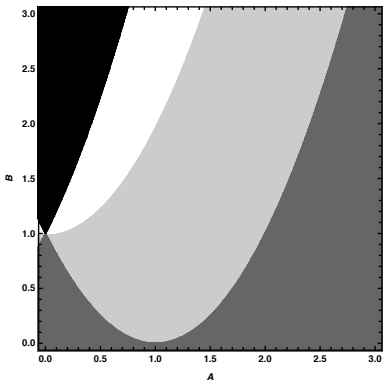

Fig. 2. N-stability and J-stability in the linear case of the Brusselator model. The white (black) region shows N-unstable and J-stable (unstable) areas. The light (dark) gray region shows N-stable and J-stable (unstable) areas.

$$G_x = 0, \tag{17}$$

$$P_x = \frac{1}{4}\left(A^2 - B + 1\right)^2 - A^2. \tag{18}$$

In a similar fashion, we rewrite Eq.(12) for x and substitute it into Eq. (11) to obtain the form $\ddot{y}+g_y = 0$. This gives the geometric quantities for y: $N_y = (1/2)(A^2-B+1)$, $G_y = 0$, and $P_y = (1/4)(A^2-B+1)^2-A^2$. Therefore, the geometric equivalence holds in the linear case: $N_x = N_y$, $G_x = G_y$, and $P_x = P_y$. Notably, these geometric quantities have no terms related to time. Thus, the types of stability for x and y remain the same, regardless of time, in agreement with the previous linear stability analysis (e.g., [Nicolis, & Prigogine, 1977; Thompson, 1982]).

3.2. *Stability around the equilibrium points*

The criterion for linear stability in Eqs. (11) and (12) is the characteristic equation $1 + A^2 - B$. The sign of this equation determines the type of linear stability. From Eq. (16), the sign of the nonlinear connection determines the linear stability. In fact, N-stability, determined by the nonlinear connection, corresponds to the linear stability around the EQPs (Fig. 1).

Let us consider the different types of stability in detail. The Brusselator model shows four types of stability, according to the parameters A and B: (i) the stable spiral ($A = 0.4, B = 0.8$), (ii) the unstable spiral ($A = 0.4, B = 1.5$), (iii) the unstable node ($A = 0.4, B = 2.1$), and (iv) the stable node ($A = 0.4, B = 0.2$).

Conversely, in KCC theory, Eqs. (16) and (18) give the N- and J-stability distributions in parametric space (Fig. 2). Based on Figs. 1 and 2, let us check the correspondence between the above results (i)∼(iv) and the N- and J-stabilities. In Fig. 2, point $(A, B) = (0.4, 0.8)$ is included in the light-gray region: N-stable and J-stable. According to Fig. 1, this combination corresponds to the stable spiral, in agreement with the above result for (i). Other points $(A, B) = (0.4, 1.5)$, $(0.4, 2.1)$, and $(0.4, 0.2)$ are included in the white (N-unstable and J-stable), black (N-unstable and J-unstable), and dark-gray (N-stable and J-unstable) regions, respectively. These results coincide with the aforementioned results for (ii)∼(iv), respectively. Moreover, the pattern shown in Fig. 2 agrees with the previous stability diagram for the Brusselator model (e.g., [Twizell *et al.*, 1999; Sarmah *et al.*, 2015]).

The Hopf bifurcation is a well-known phenomenon in the Brusselator model. In KCC theory, when the system shows Hopf bifurcation, its N-stability is neutral [Yamasaki & Yajima, 2013]. When the Brusselator model is N-neutral ($N_x = 0$), Eqs. (16) and (18) give $P_x = -A^2 < 0$, i.e., J-stable. The combination of N-neutral and J-stable corresponds to the center, as shown in Fig. 1, and $B = A^2 + 1$ gives the boundary between the white and light-gray regions in Fig. 2. The other boundaries in Fig. 2 are now given by $B = (A \pm 1)^2$ from $P_x = 0$.

In this section, we have shown that the type of KCC stability in the linear case of the Brusselator model corresponds to the previous analysis, i.e., the linear stability analysis around the EQPs. In the next

section, we will show that the stability in the nonlinear case of the Brusselator model is closely related to the stability in the non-equilibrium region.

4. KCC analysis: nonlinear case of the Brusselator model

4.1. *Geometric quantities*

In this section, the KCC stability of the Brusselator model will be considered in the nonlinear case. As described in Sec. 1, the model including the nonlinear term is given by

$$\dot{x} = (B-1)x + A^2 y + \frac{Bx^2}{A} + 2Axy + x^2 y, \tag{19}$$

$$\dot{y} = -Bx - A^2 y - \frac{Bx^2}{A} - 2Axy - x^2 y. \tag{20}$$

Following the method described in Sec. 2.1, the single second-order differential equation is derived by combining the two first-order differential equations (19) and (20). First, we rewrite (19) for y:

$$y = \frac{-ABx + A\dot{x} + Ax - Bx^2}{A(A+x)^2}. \tag{21}$$

Substitution of Eq. (21) into Eq. (20) leads to

$$\ddot{x} + g_x(x, \dot{x}) = 0, \tag{22}$$

with

$$g_x = \frac{\left(-A(B-1) + (A+x)^3 - (B+1)x\right)\dot{x} + x(A+x)^3 - 2\dot{x}^2}{A+x}. \tag{23}$$

Since g_x can be obtained, Eqs. (9), (10) and (8) give the geometric quantities of the Brusselator model in the nonlinear case:

$$N_x = \frac{-A(B-1) + (A+x)^3 - (B+1)x - 4\dot{x}}{2(A+x)}, \tag{24}$$

$$G_x = -\frac{2}{A+x}, \tag{25}$$

$$P_x = \frac{p_x}{4(A+x)^2}, \tag{26}$$

with

$$\begin{aligned} p_x = x\left(2A\left(3A^4 - 2A^2(2B+3) + B^2 - 1\right) + x\left(15A^4 + x\left(x\left(15A^2 + 6Ax - 2(B+3) + x^2\right) + 4A\left(5A^2 - 2B - 5\right)\right)\right.\right. \\ \left.\left. - 12A^2(B+2) + (B+1)^2\right)\right) + A^2\left(A^4 - 2A^2(B+1) + (B-1)^2\right) - 4\left(A^3 + 3A^2x + 3Ax^2 - A + x^3\right)\dot{x}. \end{aligned} \tag{27}$$

Compare with the linear case in which the geometric quantities are constant (Eqs. (16), (17) and (18)); these geometric quantities include the terms x and $\dot{x}$. Especially, the term $\dot{x}$ indicates that the dynamics of the non-equilibrium region affect stability in the nonlinear case. It is therefore necessary to examine stability in the non-equilibrium region to determine that in the nonlinear case. We will consider this issue in the next section.

In the same way as the derivation of Eqs. (24) and (26), we can derive N_y and P_y from $\ddot{y} + g_y(y, \dot{y}) = 0$ as follows:

$$N_y = \frac{n_y}{4\sqrt{A}(Ay+B)^2\sqrt{AB^2 - 4(Ay+B)\dot{y}}}, \tag{28}$$

with

$$n_y = -4A^3y^3\left(A-3\dot{y}\right)+B^2\left(AB\left(A^2-2B-2\right)-6\left(A^2-2B\right)\dot{y}\right)+\sqrt{A}\sqrt{AB^2-4(Ay+B)\dot{y}}\left(B\left(\left(A^2+4\right)B\right.\right.$$
$$\left.\left.-4A\dot{y}\right)+4A^2y^2-4Ay\left(A\dot{y}-2B\right)\right)-2ABy\left(3\left(A^2-6B\right)\dot{y}+2AB(B+2)\right)-2A^2By^2\left(A(B+5)-18\dot{y}\right), \tag{29}$$

and

$$P_y = \frac{p_{y1}\sqrt{AB^2-4\dot{y}(Ay+B)}+p_{y2}\sqrt{A}}{8A(Ay+B)^4\left(AB^2-4\dot{y}(Ay+B)\right)^{3/2}}, \tag{30}$$

with

$$p_{y1} = A^2\left(2A^2B^4y^2\left(A^2(-(B-3))+6B^2-28B+102\right)+4A^3B^3y^3\left(A^2+2(B-8)B+74\right)+2A^4((B-18)B\right.$$
$$+127)B^2y^4-4AB^5y\left(B\left(A^2-2B+6\right)-20\right)+B^6\left(-2A^2(B+1)+A^4+2(B-2)B+14\right)$$
$$\left.-8A^5(B-15)By^5+24A^6y^6\right)-2\dot{y}(Ay$$
$$+B)^2\left(\dot{y}\left(A^4\left(5B^2+12By^2-12y^4\right)+12A^2B^2\left(B-6y^2\right)+24A^3By\left(B-2y^2\right)-48AB^3y-12B^4\right)\right.$$
$$-2A(Ay+B)\left(B^2\left(A^2(2B+5)-2\left(B^2+B+4\right)\right)-2A^2(B+1)(B+4)y^2\right.$$
$$\left.\left.+2ABy\left(A^2-2B(B+2)-8\right)-4A^3y^3\right)\right), \tag{31}$$

$$p_{y2} = 16A\left(\dot{y}\right)^3(Ay+B)^3\left(A^2\left(B+2y^2\right)+4ABy+2B^2\right)-12\left(\dot{y}\right)^2(Ay+B)^2\left(2A^2\left(A^2+24\right)B^2y^2+4A\left(A^2\right.\right.$$
$$\left.+8\right)B^3y+B^3\left(2\left(A^2+4\right)B+A^4\right)+32A^3By^3+8A^4y^4\right)-2A\dot{y}(Ay$$
$$+B)\left(-6A^2B^3y^2\left(A^2(B-2)+12B+56\right)+8A^3B^2y^3\left(A^2-6(B+8)\right)-12AB^4y\left(\left(A^2+4\right)B+12\right)\right.$$
$$+B^5\left(-2A^2(3B+2)+A^4-12(B+2)\right)-12A^4(B+18)By^4$$
$$\left.-48A^5y^5\right)+A^2B^2\left(-2A^2B^3y^2\left(A^2(B-3)+84\right)+4A^3\left(A^2-48\right)B^2y^3-4AB^4y\left(A^2B+18\right)\right.$$
$$\left.+B^5\left(-2A^2(B+1)+A^4-12\right)-108A^4By^4-24A^5y^5\right). \tag{32}$$

N_y and P_y contain the square root term: $\sqrt{AB^2-4\dot{y}(Ay+B)}$. This term is always a real number, because Eq. (20) gives $AB^2-4\dot{y}(Ay+B)=[2x(Ay+B)+A(2Ay+B)]^2/A>0$.

In Section 3.1, we show that the equivalency, $N_x = N_y$ and $P_x = P_y$, holds in the linear case. On the other hand, the comparison of Eqs. (24) and (28), (26), and (30) shows that the equivalency does not hold in the nonlinear case. As described above, the linear case reflects the stability around the EQP, whereas the nonlinear case reflects the stability in the non-equilibrium region. Therefore, the above non-equivalency means that the stability of x and y is generally different, and agreement is limited to the EQP. Let N_E and P_E be the nonlinear connection and deviation curvature of the equilibrium state, respectively: $\dot{x}=\dot{y}=0$, their concrete forms are given by $N_E = (1/2)\left(A^2-B+1\right)$ and $P_E = (1/4)\left(A^4-2A^2B-2A^2+B^2-2B+1\right)$. For example, Fig. 3 shows the four types of curves in which N_x, N_y and P_x, P_y are equal to N_E and P_E, respectively, in the case of $A=1$ and $B=1.5$. The four curves intersect at various points, but they all coincide at the EQP; as such, one type of stability is sufficient for the EQP, i.e., a stable spiral in $A=1$ and $B=1.5$. The same result holds for the other parameters.

4.2. *Stability in the non-equilibrium region*

To visualize the distribution of the stability types in the non-equilibrium region, we consider the geometric quantities in (x,y)-space. Substitution of Eq. (19) into Eqs. (24) and (26) leads to

$$N_x = \frac{1}{2A(A+x)}\left[x^2\left(3A^2-4Ay-4B\right)+Ax\left(3A^2-8Ay-5B+3\right)+A^2\left(A^2-4Ay-B+1\right)+Ax^3\right], \tag{33}$$

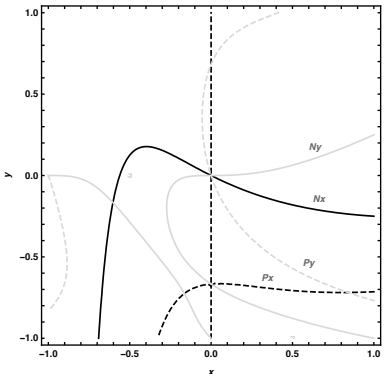

Fig. 3. Four types of curves in which N_x, N_y and P_x, P_y are equal to N_E and P_E, respectively in the case of $A = 1$ and $B = 1.5$. N_E and P_E are the nonlinear connection and deviation curvature of the equilibrium state: $\dot{x} = \dot{y} = 0$. The four curves intersect at various points, but they all coincide at the EQP (0,0)

and

$$P_x = \frac{1}{4A(A+x)^2}\left[x^5\left(6A^2-4Ay-4B\right)+Ax^4\left(15A^2-20Ay-18B-2\right)+4A^2x^3\left(5A^2-10Ay-8B-2\right)\right.$$
$$+Ax^2\left(15A^4-40A^3y-4A^2(7B+3)+4Ay+B^2+6B+1\right)$$
$$+2A^2x\left(3A^4-10A^3y-2A^2(3B+2)+4Ay+B^2+2B-3\right)$$
$$\left.+A^3\left(A^4-4A^3y-2A^2(B+1)+4Ay+(B-1)^2\right)+Ax^6\right]. \tag{34}$$

Equations (33) and (34) describe Fig. 4, which shows the stability pattern in the non-equilibrium region for the following four cases (Section 3.2): (a) $A = 0.4, B = 0.8$; (b) $A = 0.4, B = 1.5$; (c) $A = 0.4, B = 2.1$; and (d) $A = 0.4, B = 0.2$. In these four cases (a)∼(d), we will consider three regions differing in distance from the EQP $(x, y) = (0, 0)$: (I) a region near the EQP (e.g., $-10^{-2} \leq x, y \leq 10^{-2}$), (II) a region at an intermediate distance from the EQP (e.g., $-5 \leq x, y \leq 5$), and (III) a region far from the EQP.

First, we consider the region near the EQP (e.g., $-10^{-2} \leq x, y \leq 10^{-2}$). In this case, the spatial distributions of N- and J-stability are uniform. There are four types of uniform distribution, which depend on the parameters. Thus, equivalences $N_x = N_y$ and $P_x = P_y$ are in agreement with the linear case (Section 3.1). The difference in gray-scale color across parameters A, B is consistent with the results obtained in the linear case (Section 3.2). To see the switch in the distribution type in the first column of Fig. 4 (near the EQP) with changes in parameters A and B, we calculated the change in the sign of the non-linear connection and deviation curvature. Alternatively, we can check this switching by referring to Fig. 2, as shown below. The stability near the EQP corresponds to the stability of the linear case described in Fig. 2. For example, when $A = 0.4$ and $B = 0.8$, Fig. 2 shows the light gray region. Therefore, the first column ($A = 0.4$, $B = 0.8$) in Fig. 4 also shows a light gray region. In the case of the other parameters A and B, the distribution change near the equilibrium point in Fig. 4 can also be checked by referring to Fig. 2.

Next, we consider the region at an intermediate distance from the EQP (e.g., $-5 \leq x, y \leq 5$) (Fig. 4). From Eqs. (33) and (34), the stability distribution of N_x and P_x can be plotted in (x, y)-space. Based on Eqs. (28) and (30), we also know the stability distribution for N_y and P_y. Figure 4 shows that the stability distribution given by N_y and P_y is not consistent with that given by N_x and P_x. This result differs from the above case near the EQP, in which $N_x = N_y$ and $P_x = P_y$. Moreover, it shows a more complex parameter-dependent pattern than the case near the EQP. This implies that the stability structure in the intermediate non-equilibrium region plays an important role in the dynamic, complex patterns of the Brusselator model.

Finally, we consider the region far from the EQP. In this case ($x, y \gg A, B$), the stability distribution is not strongly dependent on the parameters and converges for x and y. The differences in parameters A and B will move the stability boundaries; however, the amount is negligible compared to the size of the coordinate system. For N_x and P_x, the areas around the first and third quadrants are white ($N_x < 0$ and $P_x < 0$), and

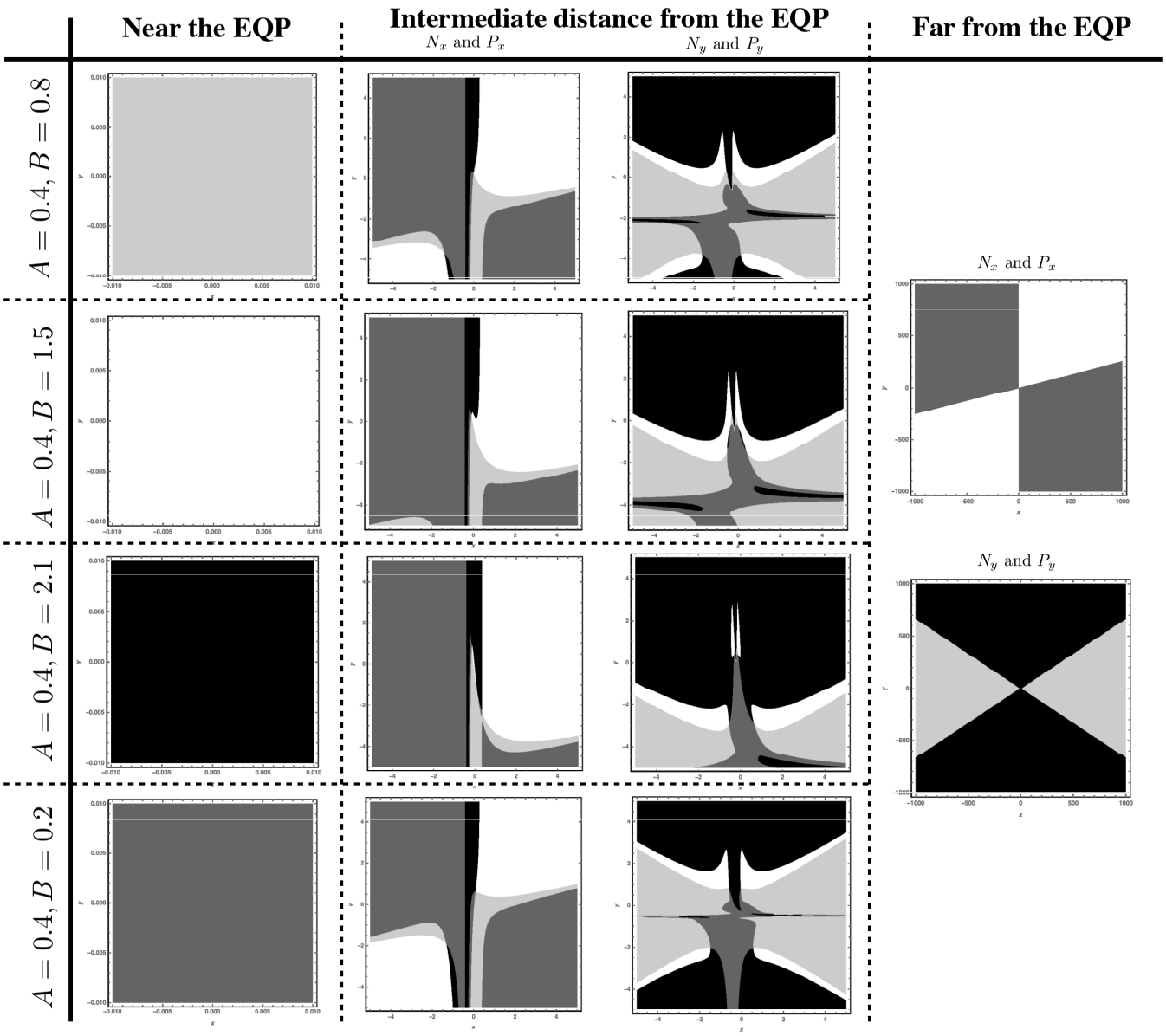

Fig. 4. Stability in the non-equilibrium region for the following four cases: $(A = 0.4, B = 0.8)$, $(A = 0.4, B = 1.5)$, $(A = 0.4, B = 2.1)$, and $(A = 0.4, B = 0.2)$. Under these four cases, we consider three regions varying in distance from the EQP $(x, y) = (0, 0)$. (I) The region near the EQP (e.g. for a plot range of $-10^{-2} \leq x, y \leq 10^{-2}$); there are four types of KCC stability patterns that show uniform distributions and parameter dependence. (II) The region at an intermediate distance from the EQP (e.g. for a plot range of $-5 \leq x, y \leq 5$).; here, various types of KCC stability patterns show non-uniform, distributions and parameter dependence. (III) The region sufficiently far from the EQP (e.g. for the plot range of $-10^3 \leq x, y \leq 10^3$) showing two types of KCC stability patterns with non-uniform and regular distributions, without parameter dependence.

those around the second and fourth quadrants are dark-gray ($N_x > 0$ and $P_x > 0$). In fact, Eqs. (33) and (34) show that $\lim_{y\to\pm\infty,x\to\pm\infty} N_x = -\infty$ and $\lim_{y\to\pm\infty,x\to\pm\infty} P_x = -\infty$; $\lim_{y\to\mp\infty,x\to\pm\infty} N_x = \infty$ and $\lim_{y\to\mp\infty,x\to\pm\infty} P_x = \infty$. In a similar fashion, we can obtain the black and light-gray patterns for N_y and P_y using the following relations: $\lim_{x\to0,y\to\pm\infty} N_y = -\infty$ and $\lim_{x\to0,y\to\pm\infty} P_y = \infty$; $\lim_{y\to0,x\to\pm\infty} N_y = \infty$ and $\lim_{y\to0,x\to\pm\infty} P_y = -\infty$.

5. Conclusions

This paper applies KCC theory to the Brusselator model and derives geometric quantities related to bifurcation phenomena. Based on these quantities, the KCC stability of the Brusselator model is analyzed in linear and nonlinear cases to determine the degree to which non-equilibrium affects bifurcation and stability. Our main conclusions are as follows.

(1) In the linear case, the geometric quantities of the Brusselator model are constant for each parameter. Here, the KCC stability is in agreement with the results of a previous linear stability analysis.
(2) In the nonlinear case, this paper considers three regions (I-III) differing in distance from the EQP. (I) In the region near the EQP, there are four distinct KCC stability patterns that show uniform distributions and parameter dependence. (II) In the region at an intermediate distance from the EQP, there are various KCC stability patterns that exhibit non-uniform, complex distributions and parameter dependence. (III) In the region far from the EQP, there are two types of KCC stability patterns that display non-uniform and regular distributions, without parameter dependence. These results indicate that the stability in the intermediate non-equilibrium region plays an important role in the dynamic complex patterns in the Brusselator model.

References

Abolghasem, H. [2012a] "Liapunov stability versus Jacobi stability," *J. Dynam. Syst. Geomet. Theo.* **10**, 13-32.

Abolghasem, H. [2012b] "Jacobi stability of circular orbits in central forces," *J. Dynam. Syst. Geomet. Theo.* **10**, 197-214.

Abolghasem, H. [2013a] "Stability of circular orbits in Schwarzschild spacetime," *IJDSDE* **12**, 131-147.

Abolghasem, H. [2013b] "Jacobi stability of hamiltonian systems," *Int. J. Pure Appl. Math.* **87**, 181-194.

Antonelli, P.L., & Kazarinoff, N.D. [1984] "Starfish predation of a growing coral reef community," *J. Theor. Biol.* **107**, 667-684.

Alawadi, M. A., Batic, D. & Nowakowski, M. [2020] "Light bending in a two black hole metric," *Class. Quantum Grav.* **38**, 045003.

Antonelli, P.L., Ingarden, R.S. & Matsumoto, M. [1993] *The Theory of Sprays and Finsler Spaces with Applications in Physics and Biology*, (Kluwer, Dordrecht).

Antonelli,, P.L. & Bucataru, I. [2003] *KCC theory of a system of second order differential equations, in: Handbook of Finsler Geometry*, (Kluwer, Dordrecht).

Antonelli, P.L., Leandro, E.S. & Rutz, S.F. [2014] "Gradient-driven dynamics on Finsler manifolds: the Jacobi action-metric theorem and an application in ecology," *Nonlinear Stud.* **21**, 141–152.

Antonelli, P. L., Rutz, S. F. & Ferreira Jr, G.S. [2019] "Remarks on modelling serial endosymbiosis and evolution of eukaryote tissue formation," *Nonlinear Stud.* **26**, 653–662.

Belousov, B.P. [1959] "An oscillating reaction and its mechanism," *Sborn. Referat. Radiat. Med.* 145–147, (Moscow: Medgiz).

Boehmer, C.G. & Harko, T., & Sabău, S.V. [2010] "Jacobi stability analysis of dynamical systems-applications in gravitation and cosmology," *ArXiv: 1010.5464*.

Cartan, E. [1933] "Observations sur le mémoire précédent," *Math. Z.* **37**, 619–622.

Chern, S.S. [1939] "Sur la géométrie d'un systéme d'équations différentielles du second ordre," *Bull. Sci. Math.* **63**, 206–212.

Chen, Y. & Yin, Z. [2019] "The Jacobi stability of a Lorenz-type multistable hyperchaotic system with a curve of equilibria," *Int. J. Bifurcat. Chaos* **29**, 1950062.

Chen, B., Liu, Y., Wei, Z. & Feng, C. [2020] "New insights into a chaotic system with only a Lyapunov stable equilibrium," *Math. Methods Appl. Sci.* **43**, 9262–9279.

Deng, Q. & Zhou, T. [2020] "Memory-induced bifurcation and oscillations in the chemical Brusselator model," *Int. J. Bifurcat. Chaos* **30**, 2050151.

Feng, C., Huang, Q. & Liu, Y. [2020] "Jacobi analysis for an unusual 3D autonomous system," *Int. J. Geom. Methods Mod. Phys.* **17**, 2050062.

Freire, J. G., Gallas, M. R. & Gallas, J. A. [2017] "Stability mosaics in a forced Brusselator," *Eur. Phys. J Spec. Top.* **226**, 1987–1995.

Gupta, M. K., & Yadav, C. K. [2017] "Jacobi stability analysis of Rössler system," *Int. J. Bifurcat. Chaos*, **27**, 1750056.

Gupta, M. K., Yadav, C. K. & Gupta, A. K. [2019] "A geometrical study of wang-chen system in view of KCC theory," *TWMS J. App. and Eng. Math.* **10**, 1064–1073.

Gupta, M. K. & Yadav, C. K. [2019] "Rabinovich-Fabrikant system in view point of KCC theory in Finsler geometry," *J. Interdiscip. Math.* **22**, 219–241.

Harko, T., Pantaragphong, P. & Sabău, S.V. [2016] "Kosambi-Cartan-Chern (KCC) theory for higher-order dynamical systems," *Int. J. Geo. Meth. Mod. Phy.* **13**, 1650014.

Huang, Q., Liu, A. & Liu, Y. [2019] "Jacobi Stability Analysis of the Chen System," *Int. J. Bifurcat. Chaos* **29**, 1950139.

Klën, W. S. & Molina, C. [2020] "Dynamical analysis of null geodesics in brane-world spacetimes," *Phys. Rev. D* **102**, 104051.

Kolebaje, O. & Popoola, O. [2019] "Jacobi stability analysis of predator-prey models with holling-type II and III functional responses," *AIP Conf. Proc.* **2184**, 060001.

Kosambi D.D. [1933] "Parallelism and path-spaces," *Math. Z.* **37**, 608–618.

Krylova, N., Voynova, Y. & Balan, V. [2019] "Application of geometrical methods to study the systems of differential equations for quantum-mechanical problems," *J. Phys. Conf. Ser.* **1416**, 012021.

Kumar, M., Mishra, T. N. & Tiwari, B. [2019] "Stability analysis of Navier-Stokes system," *Int. J. Geom. Methods Mod. Phys.*, **16**, 1950157.

Lake, M.J. & Harko, T. [2016] "Dynamical behavior and Jacobi stability analysis of wound strings," *Eur. Phys. J.* **76**, 1–26.

Lavrova, A. I., Postnikov, E. B. & Romanovsky, Y. M. [2009] "Brusselator an abstract chemical reaction?," *PHYS-USP* **52**, 1239–1244.

Liu, A., Chen, B. & Wei, Y. [2020] "Jacobi analysis of a segmented disc dynamo system," *Int. J. Geom. Methods Mod. Phys.* **17**, 2050205.

Liu, Y., Huang, Q. & Wei, Z. [2021] "Dynamics at infinity and Jacobi stability of trajectories for the Yang-Chen system," *Discrete. Contin. Dyn. Syst. Ser. B* **26**, 3357-3380.

Luo, A. C. & Guo, S. [2018] "Period-1 evolutions to chaos in a periodically forced Brusselator," *Int. J. Bifurcat. Chaos* **28**, 1830046.

Ma, M. & Hu, J. [2014] "Bifurcation and stability analysis of steady states to a Brusselator model," *Appl. Math. Comput.* **236**, 580–592.

Neagu, M. [2013] "Multi-time Kosambi-Cartan-Chern invariants and applications," *BSG Proceedings.* **20**, 36–50.

Nicolis, G. & Prigogine, I. [1977] *Self-Organization in Nonequilibrium Systems* (John Wiley & Sons, New York).

Oiwa, S. & Yajima, T. [2017] "Jacobi stability analysis and chaotic behavior of nonlinear double pendulum," *Int. J. Geom. Methods Mod. Phys.* **14**, 1750176.

Prigogine, I. & Lefever, R. [1968] "Symmetry breaking instabilities in dissipative systems. II," *J. Chem. Phys.* **48**,1695-1700.

Qin, B. W., Chung, K. W., Algaba, A. & Rodríguez-Luis, A. J. [2020] "High-order analysis of canard explosion in the Brusselator equations," *Int. J. Bifurcat. Chaos* **30**, 2050078.

Rech, P. C. [2019] "Nonlinear Dynamics of Two Discrete-Time Versions of the Continuous-Time Brusselator Model," *Int. J. Bifurcat. Chaos* **29**, 1950142.

Sabău, S.V. [2005a] "Some remarks on Jacobi stability," *Nonlinear Anal. TMA.* **63**, e143–e153.

Sabău, S.V. [2005b] "Systems biology and deviation curvature tensor," *Nonlinear Anal. RWA.* **6**, 563–587.
Salnikova, T. V., Kugushev, E. I. & Stepanov, S. Y. [2020] "Jacobi Stability of a Many-Body System with Modified Potential," *Doklady Mathematics* **101**, 154–157.
Sarmah, H. K., Das, M. C. & Baishya, T. K. [2015] "Hopf bifurcation in a chemical model," *Int. J. Innov. Res. Sci. Eng. Technol.* **1**, 23–33.
Sulimov, V. D., Shkapov, P. M. & Sulimov, A. V. [2018] "Jacobi stability and updating parameters of dynamical systems using hybrid algorithms," *IOP Conf. Ser. Mater. Sci. Eng.* **468**, 012040.
Thompson, J.M.T. [1982] *Instabilities and Catastrophes in Science and Engineering* (John Willy & Sons, New York).
Twizell, E. H., Gumel, A. B. & Cao, Q. [1999] "A second-order scheme for the "Brusselator" reaction-diffusion system," *J. Math. Chem.* **26**, 297–316.
Taylor, A. F. [2002] "Mechanism and phenomenology of an oscillating chemical reaction," *Prog. React. Kinet. Mec.* **27**, 247–326.
Udrişte, C. & Nicola, I.R. [2009] "Jacobi stability of linearized geometric dynamics," *J. Dynam. Syst. Geomet. Theo.* **7**, 161–173.
Yamasaki, K. & Yajima, T. [2013] "Lotka-Volterra system and KCC theory: Differential geometric structure of competitions and predations," *Nonlinear Anal. RWA.* **14**, 1845–1853.
Yamasaki, K. & Yajima, T. [2016] "Differential geometric structure of non-equilibrium dynamics in competition and predation: Finsler geometry and KCC theory," *J. Dynam. Syst. Geomet. Theo.* **14**, 137–153.
Yamasaki, K. & Yajima, T. [2017] "KCC analysis of the normal form of typical bifurcations in one-dimensional dynamical systems: geometrical invariants of saddle-node, transcritical, and pitchfork bifurcations," *Int. J. Bifurcat. Chaos*, **27**, 1750145.
Yamasaki, K. & Yajima, T. [2020] "KCC analysis of a one-dimensional system during catastrophic shift of the Hill function: Douglas tensor in the nonequilibrium region," *Int. J. Bifurcat. Chaos*, **30**, 2030032.
Zhabotinsky, A. M. [1964] "Periodical oxidation of malonic acid in solution (a study of the Belousov reaction kinetics)," *Biofizika* **9** 306–311.
Zhao, Z. & Ma, R. [2019] "Local and global bifurcation of steady states to a general Brusselator model," *Adv. Differ. Equ.* **No. 491** 1–14.